Geochemistry, Geophysics, Geosystems

RESEARCH ARTICLE
10.1029/2018GC008102

Badly Behaved Detrital (U-Th)/He Ages: Problems With He Diffusion Models or Geological Models?

Matthew Fox[1], **Jin-Gen Dai**[2], **and Andrew Carter**[3]

[1]London Geochronology Centre, Department of Earth Sciences, University College London, London, UK, [2]State Key Laboratory of Biogeology and Environmental Geology, School of Earth Science and Resources, and Research Center for Tibetan Plateau Geology, China University of Geosciences, Beijing, China, [3]London Geochronology Centre, Department of Earth Sciences, Birkbeck College, London, UK

Key Points:
- A radiation damage control on detrital apatite (U-Th)/He ages does not require positive correlations between age and effective uranium
- Effective uranium is a proxy for radiation damage, but interpretations must account for the complete thermal history
- Not accounting for prior history increases the potential to incorrectly attribute diffusivity variations on chemical compositions

Correspondence to:
M. Fox,
m.fox@ucl.ac.uk

Citation:
Fox, M., Dai, J.-G., & Carter, A. (2019). Badly behaved detrital (U-Th)/He ages: Problems with He diffusion models or geological models?. *Geochemistry, Geophysics, Geosystems*, *20*, 2418–2432. https://doi.org/10.1029/2018GC008102

Received 26 NOV 2018
Accepted 5 APR 2019
Accepted article online 23 APR 2019
Published online 25 MAY 2019

Abstract Dispersion in apatite (U-Th)/He ages makes extracting thermochronological information challenging. This is particularly problematic for constraining the thermal history of sedimentary basins, as the total amount of heating during burial can be small and at the limits of the sensitivity of the apatite (U-Th)/He system in apatite, but undetectable with other thermochronometric systems. Here we explore the importance of the differences in predepositional thermal histories for individual crystals and the effect of radiation damage-related diffusion during both the predepositional and postdepositional thermal history on the dispersion of apatite (U-Th)/He ages. Different predepositional thermal histories can lead to a large spread of detrital ages due to radiation damage and its effect on He diffusivity. The resulting ages may appear scattered, and relationships between age and [eU], a conventional proxy for accumulated radiation damage, may be nonexistent or nonsensical. Furthermore, other variables that are expected to control He diffusivity could vary as a function of source region, resulting in false conclusions about controls on He diffusivity and the applicability of the apatite (U-Th)/He system in general. We suggest that in some situations in which detrital apatite (U-Th)/He age does not correlate with [eU], it is not because of problems with the thermochronometric system, but problems with the assumed geological model.

1. Introduction

Extracting the thermal history of sedimentary rocks is helpful when studying landscape evolution and tectonics. In most cases, sedimentary rocks now exposed at the surface are deposited in sedimentary basins from a wide range of source areas, buried, heated and lithified, and then exhumed to the surface due to erosion and tectonics. The clearest example of this process is found in foreland sedimentary basins, and the thermal histories of these basins have been considered a unique method to provide constraints on the growth and evolution of mountain belts (Sinclair et al., 1991). Within this framework, accommodation space is created as mountainous topographic loads warp the lithosphere, forming a foreland basin in which sediments are buried and heated. As thrust faults propagate into the foreland basin, rock uplift occurs, leading to erosion and cooling. Thermal histories of foreland basins allow this transition from heating to cooling to be mapped in space and time, enabling the width and areal extent of mountain ranges to be inferred. In many cases, however, this is challenging since the low-temperature history associated with burial and exhumation within foreland basins is challenging to detect with existing thermochronometric systems.

The apatite (U-Th)/He thermochronometric system is sensitive to low temperatures (down to ~50 °C; Zeitler et al., 1987; Wolf et al., 1996) and has the potential to provide the tightest constraints on the history of sedimentary rocks. It has been argued that (U-Th)/He age dispersion makes the routine application of this approach challenging (Green & Duddy, 2018). However, several factors may explain dispersion: U and Th rich microinclusions within apatite crystals that increase ^{4}He concentration within the crystal but are not dissolved, and thus, the ^{4}He is parentless, and ages are overestimated (Fitzgerald et al., 2006; Vermeesch et al., 2007); heterogeneous ^{4}He implantation from external crystals also leads to parentless ^{4}He (Gautheron et al., 2012; Murray et al., 2014; Spiegel et al., 2009); variable patterns of U and Th zonation leads to a distribution of ^{4}He atoms due to the long-stopping distances of alpha particles (Farley et al., 1996) and is often not appropriately accounted for using a uniform distribution for an alpha-ejection factor (Farley et al., 2011; Hourigan et al., 2005); not accounting for the possibility of analyzing broken crystals results in the potential to measure younger or older ages due to sampling just part of the diffusive profile of ^{4}He within

a crystal, and this is exacerbated in sedimentary samples where abrasion of apatite crystals during sedimentary transport may remove just the outer, most diffusive, part of the crystal (Beucher et al., 2013; Brown et al., 2013); trapping of He in microvoids within apatite crystals randomly modifies diffusion kinetics resulting in dispersion (McDannell et al., 2018; Zeitler et al., 2017), apatite crystal composition (Djimbi et al., 2015), and radiation damage that influences ^{4}He diffusivity at a specific temperature (Green et al., 2006; Shuster et al., 2006) and varies as a function of crystal chemistry (Gautheron et al., 2013; Powell et al., 2018). The relative importance of these contributing factors, however, is poorly understood, reflecting in part the inability to diagnose reliably their contributions in observed data. In the case of radiation damage control on apatite (U-Th)/He ages, a diagnostic pattern of apatite (U-Th)/He ages is predicted and failure to observe such a pattern may be interpreted that radiation damage is relatively unimportant. However, we suggest that a poorly defined, or dispersed, age-[eU] relationship does not mean the data are not coherent. Here, we build on previous work (Cecil et al., 2014; Fillon et al., 2013) and highlight an alternative consequence of radiation damage, and its temperature sensitivity, on apatite (U-Th)/He ages that helps explain dispersed data from sedimentary basins.

Radiation damage refers to damage to the crystal lattice produced by products of radioactive decay and influences He diffusion kinetics and thus the sensitivity of the system to temperature (Gerin et al., 2017; Green et al., 2006; Shuster et al., 2006). In turn, different crystals that have slightly different amounts of radiation damage will transition from an open to closed thermochronometric system at different temperatures and record different thermochronometric ages. Radiation damage accumulates due to daughter recoil from intermediate alpha decays as U and Th decay to Pb, the impacts through atomic stopping of these alpha particles, and due to energetic fragments produced by spontaneous fission events. The damage to the crystal lattice changes the energetic environment along diffusion pathways, resulting in local damaged regions of the lattice in which He is preferentially sited, termed "traps" (Shuster et al., 2006). The additional energetic terms required for He atoms to escape these traps causes the apparent He diffusivity at a specific temperature to decrease over time (Shuster et al., 2006). At sufficiently high temperatures, damage sites anneal, and He diffusivity has been measured to return to higher values at a specific temperature (Shuster & Farley, 2009). Two factors control the accumulation and annealing of radiation damage in apatite and zircon. First, a higher effective uranium concentration (or [eU] = [U]+0.24[Th], which weights the U and Th concentrations according to their relative alpha particle productivity; Flowers et al., 2009; Gastil et al., 1967), will cause a higher rate of radiation damage accumulation (Flowers et al., 2009; Gautheron et al., 2009) than in samples with lower [eU]. Second, the entire thermal history the crystal has experienced will influence both radiation damage accumulation and annealing, since damage is accumulated at low temperatures (<~120 °C) but is lost or annealed at higher temperatures in apatite (Cecil et al., 2014; Fox & Shuster, 2014).

Of these two controls on radiation damage and accumulation, the most commonly reported evidence for radiation damage control on He diffusivity, and thus (U-Th)/He age dispersion, is due to differences in [eU]. In particular, radiation damage sensitivity produces diagnostic "apatite (U-Th)/He age-[eU] correlations" for crystals that have experienced the same thermal history but have different [eU] values (e.g., Ault et al., 2009; Fillon et al., 2013; Flowers et al., 2009; Flowers, 2009; Gautheron et al., 2013). This evidence for radiation damage control on He diffusivity has also been observed for intracrystal zones of different [eU] through step degassing experiments (Fox et al., 2014; Fox et al., 2017). In these cases, the crystals, or zones, with high [eU] evolve to be more retentive of He, at a specific temperature, and these crystals will be older for a given thermal history.

The alternative control on radiation damage, due to the entire thermal history, has received less attention, in part, because it is difficult to identify. Fillon et al. (2013) showed that the predepositional cooling history of apatite crystals in a detrital sample from the Southern Pyrenean foreland basin can considerably influence the measured apatite (U-Th)/He ages as well as the inferred postdepositional temperature history. Cecil et al. (2014) showed that for samples that experienced burial and reheating in the San Joaquin Basin, California, a spread of apatite (U-Th)/He ages is expected if the crystals resided at surface temperatures for different durations. These predepositional cooling histories allow crystals of the same [eU] to evolve different amounts of radiation damage, and thus, a range of ages for a specific [eU] is predicted despite identical postdepositional burial conditions. Fox and Shuster (2014) showed that in order to explain ^{4}He/^{3}He data from Grand Canyon, along with geological constraints on canyon incision and burial

temperatures from apatite fission track analyses, the predepositional thermal history needs to allow crystals to reside at low temperatures for a long period of time prior to burial to allow radiation damage to accumulate.

Some degree of age dispersion caused by radiation damage, in spite of constant average [eU] between crystals from the same sample, is also expected due to spatial variations in [eU] (Ault & Flowers, 2012). This is because zones within crystals evolve different amounts of radiation damage and thus variable temperature sensitivity (Ault & Flowers, 2012; Fox et al., 2014). Ault and Flowers (2012) showed that the expected degree of this effect for a suite of zonation measurements is relatively small (~15%) compared to the dispersion often found in sedimentary rocks (>100%). It is important to note however that there is the potential that the degree of dispersion predicted by Ault and Flowers (2012) may be slightly underestimated due to the averaging introduced during collection of LA-ICPMS data to produce maps of [eU] (Fox et al., 2017) and the conversion of 2-D maps of [eU] to radially symmetrical models (Fox et al., 2014).

Here we explore the importance of a range of predepositional cooling histories on the distribution of apatite (U-Th)/He ages. In turn, a pattern of (U-Th)/He age is expected in which age varies due to both [eU] and earlier thermal history. In a typical thermochronometric study, the number of single-crystal ages may be insufficient to fully resolve this pattern, and thus, the data may appear scattered or overdispersed with respect to simplistic model assumptions. Furthermore, groups of apatite crystals may be from different lithological units, with different chemical compositions: Plotting age against composition may yield convincing correlations; however, this might be due to disparate predepositional cooling histories as opposed to a compositional control on He diffusion kinetics. We explored the impacts of these potential variables with numerical models and a natural example from the Western Alps.

2. Methods

We use a numerical model to simulate a simple scenario in which sediment is sourced from two different parts of an orogenic belt with different exhumation, and thus cooling, rate histories. In particular, one area has rapid exhumation rates, and the other area has much slower exhumation rates. This could be due to rivers transporting detrital material from both the footwall and hanging wall of large fault zones, Figure 1 a. We simplify the problem and specify linear cooling rates to approximate steady state exhumation. Crystals are then deposited and buried immediately to an intermediate depth, which corresponds to a temperature that leads to partial degassing and partial annealing of radiation damage, before being re-exhumed. We simulate this as a linear increase in temperature followed by cooling at a constant rate to the present surface temperature, Figure 1b.

Thermal histories can therefore be defined with a predepositional cooling rate, a depositional age (t_d) and temperature condition corresponding to surface temperatures, the maximum burial temperature (T_B) at a time in the past of t_B Ma. The thermal histories begin at a time in the past that is determined based on the depositional age, the predepositional cooling rate, and the requirement that the temperature at the initial time is greater than the sensitivity range of the (U-Th)/He system, 150 °C. For example, if the predepositional cooling rate is 10 °C/Ma and the surface temperature is 0 °C, the time-temperature paths would begin at t_d + 150 (°C) /10 (°C/Ma) million years ago.

For each thermal history considered, we calculate a range of ages for a specific range of eU concentrations. We use a spherical geometry with a radius of 100 microns for each crystal and accounted for radiation damage control on He diffusion in apatite using Radiation Damage Accumulation and Annealing Model (RDAAM) (Flowers et al., 2009) and report uncorrected ages throughout. Radiation damage may be more resistant to thermal annealing than previously reported (Fillon et al., 2013; Fox et al., 2017; Fox & Shuster, 2014; Gautheron et al., 2013; Green et al., 2006; Winn et al., 2017), and this sensitivity can be modified through the fitted dimensionless parameter *rmr*0 (Flowers et al., 2009). For the synthetic examples, we used the canonical value of *rmr*0 = 0.83 and a lower value of *rmr*0 = 0.75 for the natural example below. We stress that additional work is required to constrain this value with more precision in the future (Green & Duddy, 2018). We solved the production-diffusion equations for radiogenic ^{4}He using the finite difference method in space and a Crank Nicholson method for time stepping (Ketcham, 2005). This approach models crystals that span a range of inherited radiation damage for a given eU concentration; the radiation damage

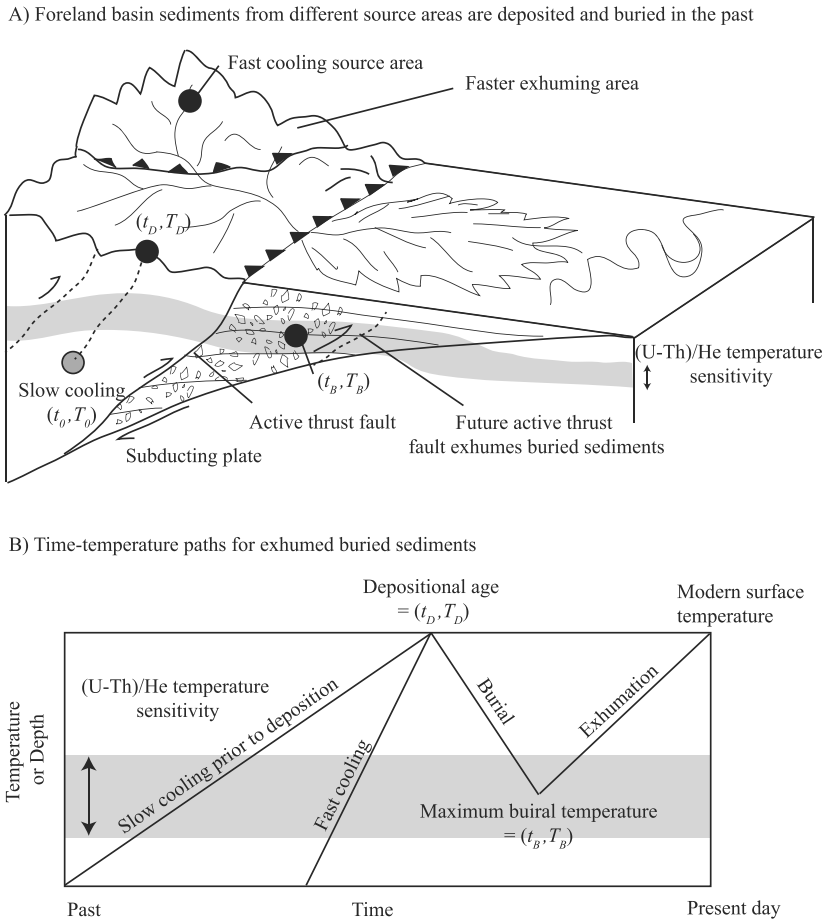

Figure 1. (a) A foreland basin was filled with sediment derived from two source regions with distinct cooling histories. At some time in the future, a new active thrust will exhume the sediments that are buried in the foreland basin. These rocks will have experienced an initial thermal history of fast or slow cooling to the surface, followed by transport and deposition in the basin at time t_D. For our analysis, we treat the transport time of sediments as a geologically instantaneous process. Sediment from both source regions will be buried to a maximum time-temperature of t_B Ma and T_B °C before being exhumed to the surface at the present day. (b) The exhumation and burial history depicted in Figure 1a is described with simple linear cooling and heating paths.

accumulated before burial directly controls the He diffusion kinetics and thus the amount of ^{4}He lost during subsequent burial reheating (Cecil et al., 2014; Fillon et al., 2013; Fox & Shuster, 2014).

For the case of zoned crystals, discussed in the example result, we solve the production-diffusion equation numerically, as above, and calculate local production rates due to the long-stopping distances of alpha particles and local radiation damage at each discrete node (Fox & Shuster, 2014; Ketcham, 2005). In order to simulate a range of crystal zonation scenarios, an inner zone is defined between the center of the crystal and a position of $R/2$ where R is the radius of the crystal. An outer zone is defined between $R/2$ and R. The [eU] values of these zones are C_1 and C_2, respectively, and the bulk value is B. For simplicity, we use a thorium concentration of 0 ppm for all numerical experiments, and therefore, [eU] is equal to [U]. In order to generate values of C_1 and C_2 that result in a specified B value, we specify a zonation ratio, $Z = C_1/C_2$, which varies between ~0.001 and 100. After writing the relative volumes of the two zones and rearranging to determine the concentration in each zone, we find that $C_1 = 8B/(1+7/Z)$ and $C_2 = 8B/(Z+7/8)$. This allows us to explore the importance of zonation on age dispersion, while keeping the bulk [eU] values constant. This is because measuring zonation is not routinely carried out; thus, a bulk [eU] value is often all that is available.

Finally, for the example result below, we draw random ages from the calculated age distributions to simulate measuring ages from an actual sample. This is to account for the fact that current methodologies are not well

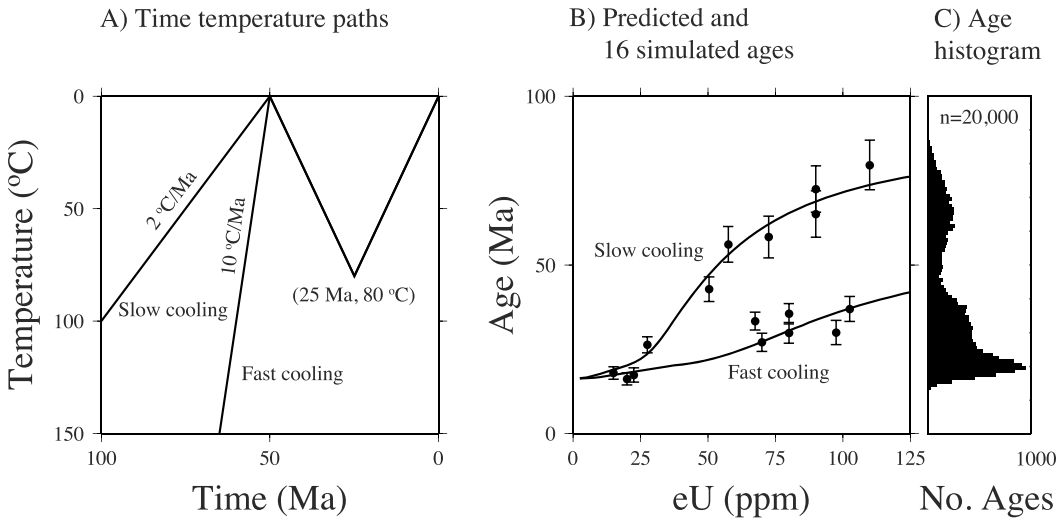

Figure 2. (a) Time-temperature paths for two different source regions that share common burial and exhumation history in a foreland basin. (b) Predicted ages for the time-temperature paths shown in Figure 2a. The slow predepositional cooling history predicts ages that are older than the faster predepositional cooling history, solid black curves. Sixteen ages are simulated by randomly sampling the calculated ages and perturbing the sampled ages using a Gaussian distribution with a standard deviation of 10% of the calculated age. Errors are assumed to be 10% of the simulated ages. (c) The probability of producing a given age is proportional to the frequency of simulating that given age. A total of 20,000 simulated ages produced using the same approach as described above yield a dominant age peak for this scenario of approximately 20 Ma.

suited to generating hundreds of ages, and thus, data sets are typically between ~5 and 30 ages per sample. Furthermore, it is not possible to target crystals of specific [eU] concentrations because U and Th are measured after crystals have been handpicked and ^{4}He has been measured. We also perturb the calculated ages to simulate measurement error. This is achieved by generating a random number from a Gaussian distribution centered on the calculated age with a standard deviation of 10% of the calculated age. This is simply to generate a data set that helps illustrate differences between true age distributions and measured ages.

3. Results

3.1. Example Result

We highlight the systematics of our model with a simple example, where the depositional age (t_D) was set to 50 Ma and the maximum burial temperature (T_B) was set to 80 °C at a time of 25 Ma (t_B; Figure 2a). Two predepositional cooling rates were modeled to simulate two distinct source regions.

The corresponding calculated age-[eU] relationships are shown for the two thermal histories along with the simulated measured ages. These ages conform to the general trend of the true calculated ages; however, there is considerable spread. This spread is due to the fact that we have randomly sampled different [eU] values and then perturbed the calculated ages as described above. This degree of spread is a not unexpected in a typical detrital (U-Th)/He data set and has been attributed to factors other than radiation damage as discussed in the introduction, Figure 2b. In addition, we simulate 20,000 ages in order to calculate the expected frequency of obtaining specific ages, Figure 2c. We see that there is a high probability of predicting young ages (~20 Ma) and there is a relatively uniform probability of predicting other ages. This highlights that there is a good chance of measuring a cluster of ages of approximately 20 Ma and an "anomalous" age or "outlier." However, this anomalous age should be expected in a detrital data set due to the effects of radiation damage and variable predepositional thermal histories. Here we have assumed that apatites from different areas have similar [eU] values. In section 4.2 we discuss some of the implications of different source regions yielding apatite crystals with different compositions and [eU] values. This could lead to strong age-[eU]

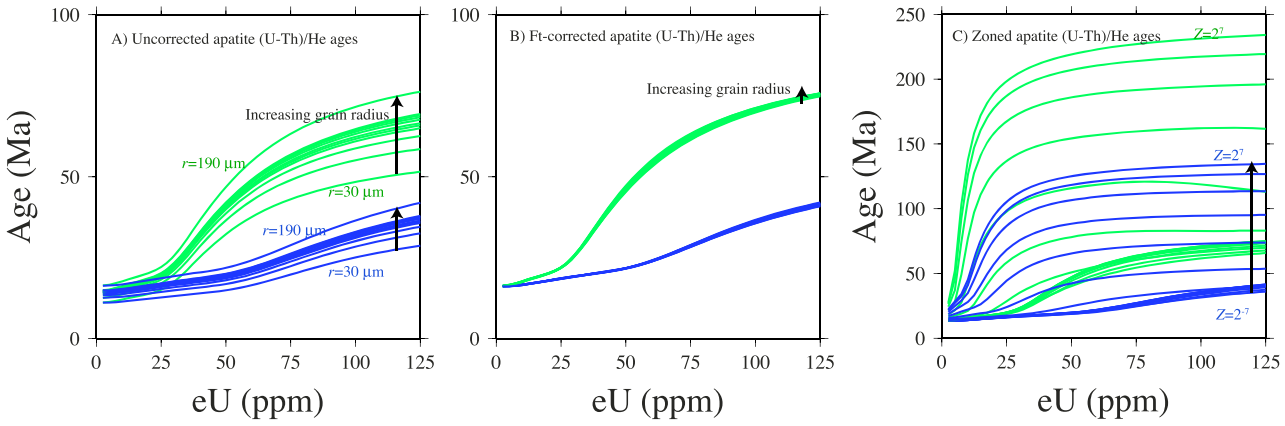

Figure 3. The effect of other potential sources of age dispersion. In all experiments, the time-temperature paths are the same as those used in Figure 2. The green predicted ages correspond to the slow-cooling predepositional time-temperature paths. The blue predicted ages correspond to the faster predepositional time-temperature path. The effects of grain size for the two different predepositional time temperature paths are shown for uncorrected ages (a) and Ft-corrected ages (b). (c) The effects of zonation is shown for a grain size of 100 microns, with Z values from 2^{-7} to 2^{7}.

correlations and weak correlations or lead to conclusions about the relative importance of chemical composition in controlling apatite (U-Th)/He age.

We use these same time-temperature paths to highlight the effects of two other causes of age dispersion. First, we calculate apatite (U-Th)/He ages for a range of grain sizes from 30 microns to 200 microns in radius. These uncorrected ages are shown in Figure 3a and the corresponding corrected ages are shown in Figure 3b. Here the correction does a very good job at reducing the age spread, as is expected (Farley, 1996).

Second, we calculate apatite (U-Th)/He ages for a range of crystal zonation variations with grain size held constant at 100 microns in radius. The zonation ratio, $Z = C_1/C_2$, varies between 2^{-7} (7.8125×10^{-3}) to 2^{7} (128), so that for Z less than one, the outer, and larger by volume, zone is enriched in uranium relative to the central zone. In contrast, when Z is large, the central zone is enriched. This results in quite extreme zonation: For a bulk concentration of 50, when Z is 2^{-7}, the outer zone has a value of 57 ppm, and the inner zone has a concentration of 0.45 ppm; when Z is 2^{7} the outer zone has a concentration of 3.0 ppm, and the inner zone has a concentration of 379.3 ppm. Importantly, for small Z values, the [eU] concentration of the larger zone is very close to the actual bulk value. However, for large Z values, the concentration values of both zones are very different from the bulk concentration value. This results in a crystal with a specific bulk [eU] value, behaving like a crystal with an [eU] value that is the same as the central zone, which can be very different. The calculated uncorrected ages are shown in Figure 3c. The correction factor does not reduce the overall spread in age because the correction factor for the crystals with a large Z value is close to unity; therefore, we do not show the corrected ages. This is because most of the helium that is produced is within the high [eU] zone and is not ejected from the crystal. These zonation values lead to a large degree of dispersion. It is important to note, however, that such large variations in zonation are unexpected for most crystals (Ault & Flowers, 2012) and this problem can be identified in apatite (U-Th)/He data sets (McKeon et al., 2014)

3.2. Varying the Burial Temperature

Building from the example result, we highlight the sensitivity of the pattern of ages to changes in the maximum burial temperature (T_B). The depositional age (t_D) was kept at 50 Ma, and the time of maximum burial was kept at 25 Ma (t_B). Here we do not simulate measured ages assuming an additional source of random dispersion; instead, we show the calculated ages. The full range of calculated ages is plotted as a function of the maximum burial temperature (Figure 4a). We see the youngest ages initially decrease as temperature increases until these youngest ages become relatively insensitive to increased temperatures. At this point, accumulated radiation damage is annealed, and He is lost through diffusion: The ages reflect the timing of cooling through the partial retention zone during cooling, and this is relatively similar for all time-temperature paths. Ages continue to increase for crystals with more radiation damage, due to either

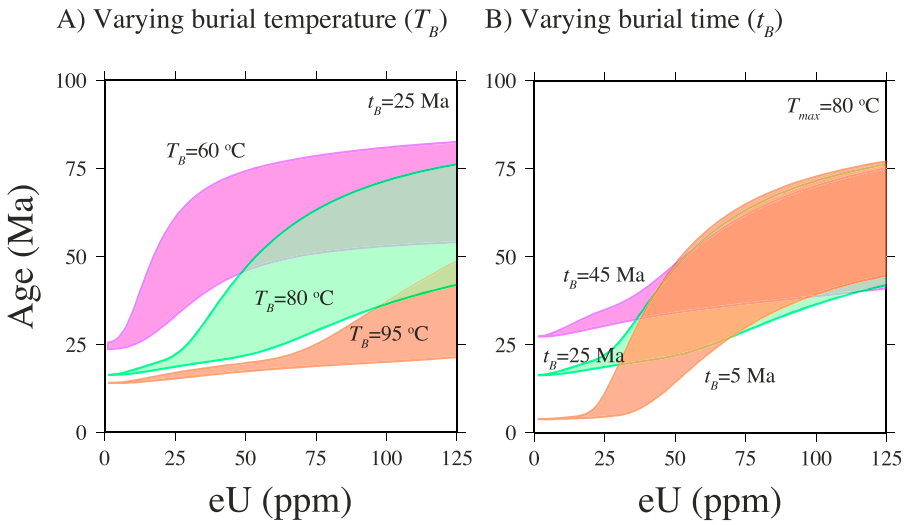

Figure 4. The effect of varying the burial conditions on the predicted spread of apatite (U-Th)/He ages. The general form of the thermal histories is the same in as in Figure 2; however, the peak burial temperature is varied in (a), and the timing of peak burial is varied in (b).

high [eU] values or slow prior cooling. In addition, the spread in age decreases as radiation damage is annealed, and more of the ^{4}He that was accumulated before deposition is lost (Ault & Flowers, 2012).

3.3. Varying the Burial Time

The example result is once again used as the basis for the analysis, and the time of maximum burial (t_B) is varied from 5 to 45 Ma. This has a clear effect on the minimum predicted age but less effect on the age range (Figure 4b). Both the age and the range in age will depend on the exact range in predepositional cooling histories. This minimum age corresponds to low amounts of radiation damage due to either low [eU] or fast cooling prior to burial. If the burial temperature is sufficiently high to diffuse all the existing ^{4}He, this age corresponds to cooling following burial. This highlights the importance of the youngest ages when making inferences from apatite (U-Th)/He ages. The general pattern of the spread in ages is relatively consistent between these simulations.

3.4. Example From the Western Alps

There has been considerable work on reconstructing the thermal history of the foreland basin sediments from the Western Alps in terms of regional exhumation in relation to climate or tectonics (e.g., Cederbom et al., 2011; Fox et al., 2015). Recently, Schwartz et al. (2017) carried out an apatite fission track and apatite (U-Th)/He analysis on samples that were buried by the Digne Nappe before being incorporated into the Alpine orogen and exhumed. The sedimentary rocks that were sampled are comprised of upper Eocene to lower Oligocene fluvial and Miocene marine molasse deposits, and Schwartz et al. (2017) used an inverse approach to constrain the burial and exhumation rate history (Gallagher, 2012). Importantly, Schwartz et al. (2017) assumed two key factors that enable this approach to recover tight constraints on the thermal history in terms of peak burial temperature and timing of peak burial: first, that crystals from the same location all experienced an identical thermal history, despite the large degree of dispersion (up to 74 %) in the Apatite Fission Track (AFT) individual ages suggesting multiple populations if more grains were counted; second, that samples from different elevations all experienced the same heating and cooling trends but offset by a specific temperature reflecting a constant geothermal gradient, despite the small differences in elevation, the expected changes in geothermal gradient during burial and exhumation, and the large amount of folding that has occurred during burial and exhumation (Figure 3: Schwartz et al., 2017). Furthermore, a single time temperature path fails to explain the large dispersion of the apatite (U-Th)/He ages (Schwartz et al., 2017). Here, we combine all the data together for the Esclangon samples from the “Vélodrôme” recumbent syncline and attempt to explain the overall trends using the recovered time-temperature path of Schwartz et al. (2017), shown in Figure 5. The measured apatite (U-Th)/He ages range from 3 to 60 Ma. The central

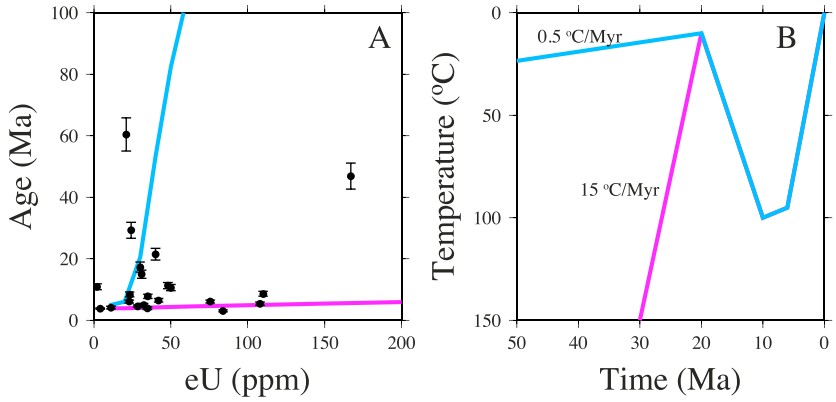

Figure 5. Natural example from the Western Alps, after Schwartz et al. (2017). (a) Corrected (U-Th)/He ages of the Esclangon samples from the "Vélodrôme" recumbent syncline (Schwartz et al., 2017). Central fission track ages (not shown) for three samples range from 11 to 62 Ma, with the lowest elevation sample corresponding to the youngest age. The colored lines correspond to predicted corrected ages with an effective spherical radius of 73 microns and cooling paths shown in Figure 4b. A value of *rmr*0 of 0.75 was used for these calculations. (b) A thermal history for the burial of the Esclangon samples after deposition and the range of expected predepositional thermal histories that apatite crystals might have experienced. The thermal history is based on the Schwartz et al. (2017). It is important to note that neither thermal history alone can explain the observed dispersion: it only by allowing for multiple thermal histories prior to deposition that the data can be explained.

age of the youngest AFT sample is 11±2 Ma with 57% dispersion (crystal ages range: 3–49, $n = 19$) and the oldest central age is 62±16 Ma with 74% dispersion (crystal ages range: 11–266 Ma, n=12); however, the number of grains is low and insufficient to adequately define the true age distribution, and thus, the central age has a large uncertainty.

We test the hypothesis that the predepositional thermal history is important for explaining the dispersion with two predepositional thermal histories: fast cooling rates of 15 °C/Myr and slow rates of 0.5 °C/Myr. It is expected that the predepositional thermal histories may be complex and therefore the modeled constant cooling rates are designed to encompass the expected average cooling rates. The slowest cooling source area is likely to be the Massif Central, where the thermal history is complex but rocks have been below 150 °C for approximately 300 Myr (Gautheron et al., 2009). The fastest cooling source areas are likely to be from the internal parts of the western Alps that were rapidly exhumed in the Late Eocene, resulting in cooling rates that were several 10 °C/Myr (Schwartz et al., 2017). These predepositional thermal histories do a reasonable job at explaining the spread in the apatite (U-Th)/He ages and result in simulated AFT ages of 14 and 71 Ma using the annealing parameters of Ketcham et al. (2007). This highlights that the data are only overdispersed if the geological model is oversimplified: by incorporating additional complexity the data can be explained. Neither time-temperature path (slow cooling or rapid cooling prior to deposition) explains the data alone, and both paths are required to explain the dispersion. However, incorporating this additional complexity that the crystals may have different predepositional cooling histories also increases the range of burial histories that will fit the data, as shown in the previous examples. Although the key components of the recovered time-temperature path presented by Schwartz et al. (2017) are likely robust, the ability of the data to constrain the time-temperature path is overestimated. It is important to note that parent nuclide zonation could also lead to the observed spread in age, as shown in section 3.1. However, there is no reported evidence for this cause of dispersion, and there is clearly geological evidence for a range of source areas, leading to dispersion.

4. Discussion

4.1. Nonuniqueness Versus No Appropriate Time-Temperature Path

The example presented in section 3 highlights that a large range, or apparent overdispersion, of ages is expected for a scenario in which detrital material is analyzed that has been sourced from multiple locations with different thermal histories. The spread of ages is not simply a function of [eU], despite the fact that this

spread is largely due to differences in radiation damage. Furthermore, extracting thermal information from this data set may be challenging. For example, HeFTy is extensively used to infer thermal histories based on a trial and error approach in which thermal histories are generated randomly (with the option to include constraints) and used to calculate (U-Th)/He ages (Ketcham, 2005). Time-temperature paths that explain the data are deemed to be good or acceptable based on the comparison between observed and predicted ages. However, if multiple ages are observed for a single [eU], a single time-temperature path will not be able to explain the data, and thus, no acceptable paths will be found (Vermeesch & Tian, 2014). This form of dispersion may be because the crystals do not share a single time-temperature path and that the geological model is too simplistic. This may lead to authors rejecting ages as outliers in order to isolate thermal histories consistent with the remaining data. In addition, there is a risk that by not accounting for the variability of predepositional thermal histories, a recovered postdepositional thermal history from an inverse algorithm may be incorrect, as has been shown for the fission track system (Carter & Gallagher, 2004).

It is important to note that this is not a problem related to nonunique solutions to the inverse problem. Problems related to nonunique solutions are highlighted with the case of a single apatite (U-Th)/He age: There are multiple time-temperature paths that will explain that age (Wolf et al., 1998) from constant temperature scenarios, to linear cooling and complex reheating thermal histories. Therefore, additional data or assumptions about the complexity of the thermal history are required to find a thermal history, and the uncertainty associated with this thermal history. In the case of data from bedrock samples, a range of time-temperature paths are consistent with the data, as in fission track analyses (Green & Duddy, 2012), and any one of these time-temperatures will explain the data. Instead, in the case of detrital samples, multiple time-temperature paths, corresponding to multiple source areas, may be required to explain the data, and a range in the bounding time-temperature paths is expected. This presents visualization challenges in that a range of time-temperature paths are required to explain the data, along with a means of showing the variability of these paths as a function of complexity and the resolving power of the data.

The nonunique relationship between time-temperature path and apatite (U-Th)/He age (Wolf et al., 1998) highlights the problem with using the "closure" temperature (Dodson, 1973). With the addition of more complex time-temperature paths, which may include reheating events, and the effect of radiation damage and annealing, the closure temperature becomes even less applicable. Therefore, it is important that other data are combined to resolve thermal histories and that numerical schemes that solve the helium production-diffusion equation, incorporating the effects of radiation damage, are used to interpret apatite (U-Th)/He ages.

It is also important to note that there may be cases where all detrital ages can be predicted within error simply by increasing the number of source areas (Fillon et al., 2013). This has important implications for inverse models in which time-temperature paths are randomly generated and predictions are compared to measurements. In general, the potential for data to constrain a thermal history depends on different aspects of the data providing different, but overlapping, information. In the case of interpreting bedrock (U-Th)/He data using the radiation damage model, different crystals have different temperature sensitivity, allowing a thermal history to be resolved in time. Importantly, each analyzed crystal has the same thermal history. In the case of detrital (U-Th)/He data and the radiation damage model, however, there is the potential that every crystal analyzed has come from a different location and has a different thermal history. The ability of these data to resolve the burial conditions may therefore be very low. This concept is clear if all detrital ages are older than the depositional age and the burial conditions resulted in limited reheating, in which some helium was lost through diffusion for some of the crystal. The degree of reheating is unresolvable because the data can be reproduced exactly, simply by changing the predeposition thermal history: A crystal that is only just older than the depositional age could be the result of partial degassing of an older crystal or rapid cooling prior to burial; a crystal that is slightly older may be the result of less diffusive loss of helium due to additional radiation damage (thereby providing constraints on burial), or it could be due to slightly slower cooling prior to burial. In turn, judging an appropriate thermal history just on the data fit is not necessarily appropriate for detrital samples. If a limited number of source areas can be defined through crystal chemistry or if additional data can be used to constrain the range of predepositional thermal histories, then there may be sufficient redundant information to infer burial conditions. This approach of defining populations of data with a common predepositional cooling rate has been implemented in the transdimensional inverse algorithm in the QTQt software (Gallagher, 2012). An alternative approach would be to treat the

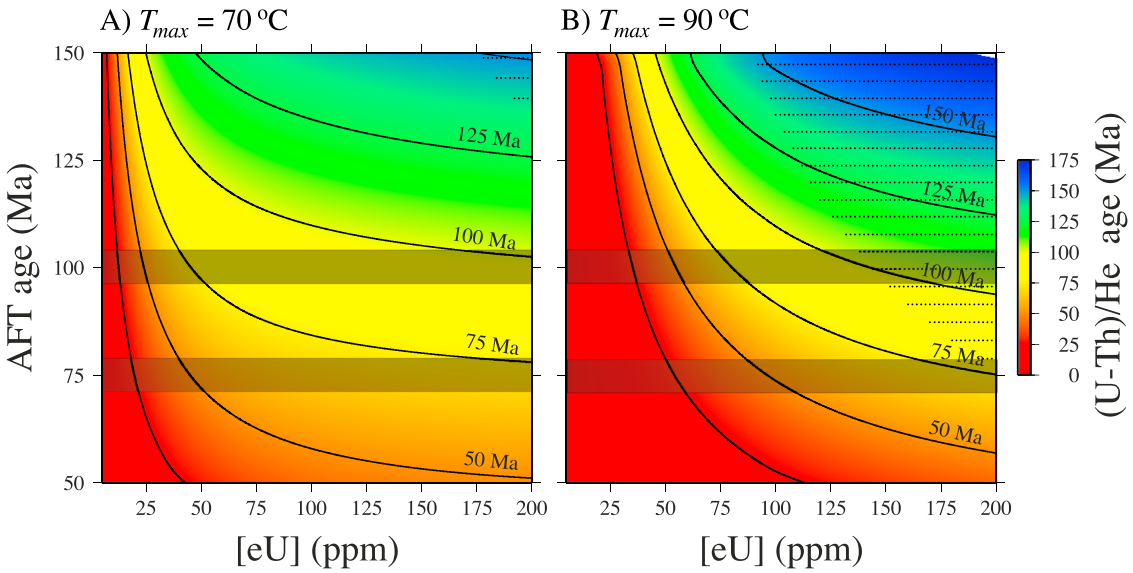

Figure 6. (U-Th)/He age as function of apatite fission track age and effective uranium for different burial temperatures of 70 °C and 90 °C in (a) and (b), respectively. The black dotted area highlights [eU] concentrations and predepositional cooling histories that lead to (U-Th)/He ages that are older than apatite fission track ages. The shaded areas highlight the range of (U-Th)/He ages that are expected if two age populations (at 75 and 100 Ma) are identified in the apatite fission age distribution. This highlights the potential to use the combination of apatite fission track and (U-Th)/He to distinguish between different burial conditions.

number of different source areas as a hyper-parameter that is sampled using the reversible jump Markov Chain Monte Carlo algorithm in QTQt.

Our results from varying the burial time and temperature highlight that recovering these conditions is challenging. Importantly, additional thermochronometric data (e.g., AFT) can be used to constrain the predepositional thermal history and thus help constrain the burial history. In particular, thermochronometric systems that will not be reset, or only partially reset, during burial will provide constraints on the predepositional thermal history, and this reduces the possible time-temperature histories that are permitted. We highlight this by plotting numerically calculated apatite (U-Th)/He ages as a function of calculated apatite fission track ages (using the annealing parameters of Ketcham et al., 2007), against [eU], Figure 6. This plot highlights the expected range of (U-Th)/He ages for a given thermal history given measured apatite fission track ages and [eU] concentrations. Different parameters (predepositional thermal history, timing of maximum burial, and temperature of maximum burial) will control the distribution of apatite (U-Th)/He age, but the apatite fission track ages will be most sensitive to the predepositional thermal history. Therefore, as other thermochronometric systems that constrain different portions of the thermal history are combined, the potential to infer complexities is increased. For example, if two apatite fission track age populations are detected at approximately 75 and 100 Ma (gray boxes in Figure 6), corresponding to different source regions, the expected apatite (U-Th)/He ages will vary as a function of burial conditions. In turn, the burial conditions can be determined by inspecting the range of (U-Th)/He ages. In this case, if the burial conditions are 70 °C, the maximum (U-Th)/He ages are approximately 100 Ma when 100-Ma apatite fission track ages are found in the sample. However, if older apatite (U-Th)/He ages are found along with 100-Ma fission track ages, higher burial temperatures are required. This uncertainty is greatly reduced if apatite crystals are "double-dated" with fission track and (U-Th)/He thermochronometry (e.g., Thomson et al., 2013). Furthermore, vitrinite reflectance data can be used to constrain the temperature conditions during burial, decreasing uncertainty further (Nielsen et al., 2017).

4.2. Misleading Correlations

Scenarios like those presented in section 3 may lead to misleading correlations. In turn, misinterpretation of these correlations may result in incorrect conclusions about how [eU] or apatite composition influence the apatite (U-Th)/He system. If apatites from the two source regions have differences in [eU], two distinct

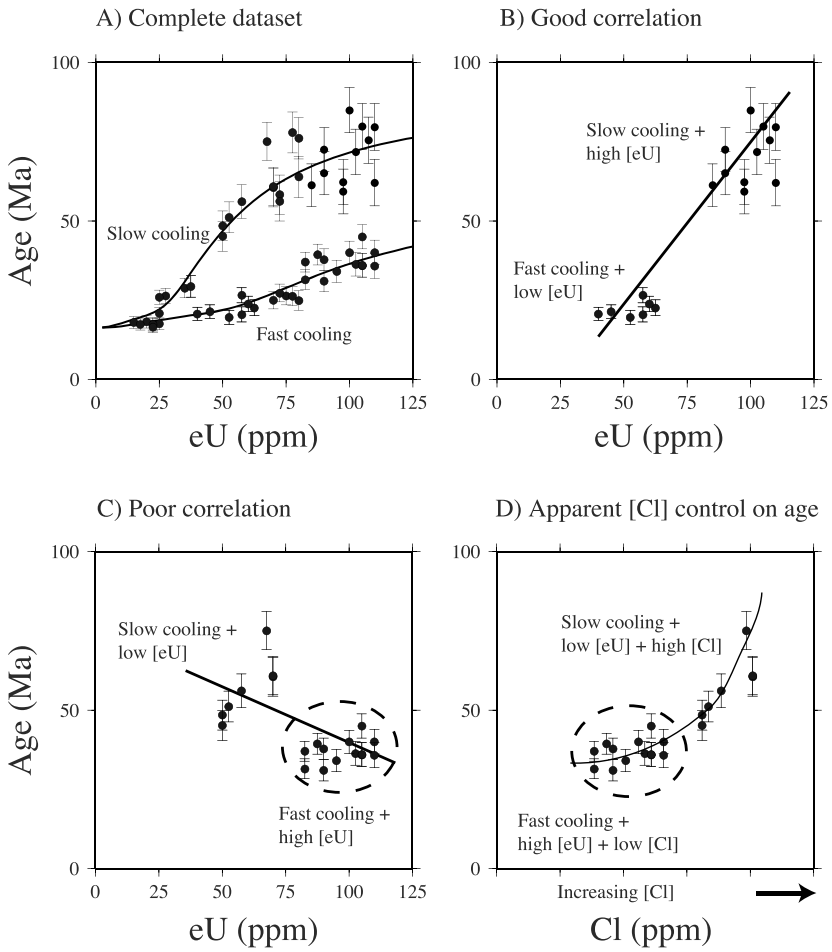

Figure 7. Potential for misleading correlations due to different source regions. (a) A complete data set of 58 ages show two characteristic age-[eU] correlations corresponding to the two thermal histories in Figure 1a. (b) If the two source regions yield apatite crystals with different chemistry, age-[eU] correlations may be good but will be spurious. In this example, the slowly cooled source region yields apatites with high [eU], and the fast-cooling source region yields apatites with low-[eU], resulting in a positive correlation between age and [eU]. If this correlation is exploited to extract thermal histories, an incorrect thermal history will be inferred. (c) The opposite scenario is also possible (slow cooling and low [eU] from one source region and fast cooling and high [eU] from the other region). This results in a poor correlation, or possibly a negative correlation, that could be incorrectly used to argue against the utility of the radiation damage model. (d) The two source regions may also produce apatite crystals with different [*Cl*] or [*F*] values. This could lead to incorrectly identifying causal relationships between age and apatite chemistry.

age-[eU] trends will be observed. We have predicted this case in Figure 7a. The solid curves are the predicted ages, and we produce a synthetic data set by randomly generating a large number (58) of ages at a range of [eU] values, which can deviate from the predicted age as described in the methodology. We then select ages from this synthetic data set to highlight that positive or negative age-[eU] correlations may be observed if a typical number of crystals are dated. For example, if the fast-cooling area correlates with low [eU] apatites, but the fast-cooling area yields apatites that have high [eU] values, a positive age-[eU] correlation is predicted. This is shown in Figure 7b where 16 ages have been selected from the predicted ages. If such a positive relationship between age and [eU] due to differences in [eU] between the source regions is observed, this would be problematic because, despite the data following an expected age-[eU] correlation (Flowers & Kelley, 2011), inferred time-temperatures paths will be inaccurate or unrealistic. In addition, the model may fit the data well and the time-temperature path may appear well resolved. If the correlations are reversed and the slow-cooling area yields low [eU] values and the fast-cooling area yields high [eU] values, a negative age-[eU] trend is possible (Figure 7c). This absence of a positive age-[eU]

correlation is possible and is predicted with a simple radiation damage model, with variable source areas. In both cases, identifying and removing outliers would lead to stronger correlations, but this would further increase the potential to infer incorrect time-temperature paths.

Additional chemical composition variability is expected to have an influence on apatite (U-Th)/He ages, either through modifying the rate of annealing of radiation damage (Gautheron et al., 2013) or modifying He diffusion pathways (Mbongo-Djimbi et al., 2015). In a dispersed data set, like the simulated data set in Figure 2b, it is common practice to attempt to determine whether a chemical composition can explain more of the variability than [eU]. We stress that care should be taken when exploring these correlations. For example, if crystals come from two source regions with different thermal histories, there may be no correlation of age with [eU], as with Figure 7c. An alternative situation is if the populations have similar [eU] values they may cluster around two distinct ages, but again, there may be no age-[eU] correlation. If these source regions yield apatites with different chlorine or fluorine content, for example, then an age-[Cl] correlation or age-[F] correlation may be identified. We highlight these ideas in Figure 7d. This is a potential scenario that could lead to incorrect conclusions about the relative importance of the radiation damage and annealing model compared to the influence of apatite chemical composition. It is therefore important to use bedrock data, where the analyzed crystals have identical thermal histories, to test the compositional controls on (U-Th)/He ages (Recanati et al., 2017).

4.3. Additional Sources of Uncertainty

We have highlighted that a large spread of apatite (U-Th)/He is expected for sedimentary rocks due to predepositional thermal histories (Fillon et al., 2013; Cecil et al., 2014). Additional dispersion in apatite (U-Th)/He age is expected due to the U and Th rich microinclusions, heterogeneous ^{4}He implantation from external crystals, variable patterns of U and Th zonation, measuring broken crystal, trapping of He in microvoids, and apatite crystal composition. Quantitative analysis of this dispersion requires that it can be mapped, which in turn requires collecting tens of crystal ages as opposed to three to five crystal ages per sample, as required for inferring time-temperature paths from broken crystals (Beucher et al., 2013; Brown et al., 2013). A promising approach the rapid acquisition of apatite (U-Th)/He ages required to map the dispersion is to measure U, Th, and He in situ, negating several time-consuming steps (Evans et al., 2015; Tian et al., 2017; Tripathy-Lang et al., 2013; Vermeesch et al., 2012). An alternative approach is to gain as much data constraining the time temperature history of individual crystals either through dating the same crystal with multiple thermochronometric systems (Thomson et al., 2013) or through mapping the spatial distribution of helium using ^{4}He/^{3}He thermochronometry (Shuster & Farley, 2004) or in situ methods (Danišík et al., 2017).

An additional source of uncertainty that we have not accounted for is the uncertainty associated with the radiation damage and annealing models. In particular, the rate at which radiation damage anneals at a specific temperature is currently relatively poorly constrained (Flowers et al., 2009; Fox & Shuster, 2014; Gautheron et al., 2013; Willett et al., 2017). Furthermore, radiation damage in apatite crystals in a single data set may behave slightly differently due to differences in chemical composition leading to further dispersion.

5. Conclusions

We have highlighted a mechanism to explain dispersion in detrital apatite (U-Th)/He data sets. This dispersion results from crystals having different degrees of radiation damage due to both differences in [eU] and predepositional cooling histories. Importantly, this dispersion may not yield strong correlations between apatite (U-Th)/He age and [eU], because this relationship does not capture differences in cooling histories leading to differences in radiation damage. Therefore, the importance of radiation damage on controlling the diffusivity of He in apatite should not be neglected simply because ages do not correlate with [eU], as has been suggested by Green and Duddy (2018). In addition, misleading age-[eU] correlations may be observed due to different source regions having differences in [eU]. More generally, this example highlights the risk of plotting apatite (U-Th)/He ages against single parameters that may influence the age, but not accounting for the multiple factors that simultaneously influence apatite (U-Th)/He ages and how these factors may covary, such as predepositional radiation damage.

By accounting for the possibility that crystals may have different predepositional thermal histories, the age dispersion can be explained, and meaningful geological information can be extracted. This is not possible if a single, and shared, thermal history is sought through inverse methods to explain the data. In some cases, this may result in the predicted data failing to fit the observations, but yielding a well-resolved thermal history. This was explored with a natural example from the Western Alps. If source areas yield apatites with different [eU] values, it may be possible to have the insidious result of an apparently well-resolved shared thermal history that also predicts the data (Figure 7b). Therefore, the result of an inverse model should not be judged solely on fit to the data, because the forward model may be incorrect if there are multiple source areas. If the forward model is modified to allow each crystal to have an independent predepositional thermal history, the ability of the data to constrain the burial history decreases. This is because the temperature sensitivity of each crystal may be different and unknown due to radiation damage accumulated during the predepositional cooling history. In turn, it is often possible to fit all the ages with a very simple forward model, without the need for inverse models. Key parameters such as the maximum burial temperature or timing of maximum burial can be inferred from these forward models.

If groups of apatite (U-Th)/He ages can be determined, then different shared predepositional thermal histories can be inferred for these groups using inverse models. In turn, it may be possible to infer predepositional thermal histories that are more complicated than those presented here, as well as detailed burial histories that are common for all groups. However, it is unclear how to group detrital apatite (U-Th)/He ages due to compositional factors that may lead to age variations and the limited number of ages that are typically measured. For example, the [Cl] of apatite crystals may be used as a means to determine apatite source or as a parameter that controls radiation damage. There is also the potential to have different inferred thermal histories for each group depending on which crystals comprise each group. Therefore, several inverse solutions should be presented to highlight sensitivity to this grouping. Any additional data in the form of depositional age constraints, vitrinite reflectance data, or additional thermochronometric ages from other systems (e.g., apatite fission track or zircon (U-Th)/He ages) will improve the reliability of the recovered thermal histories. In addition, data that constrain a continuous period of the thermal history of a single crystal could be incorporated into forward and inverse models. These data could be in the form of $^{4}He/^{3}He$ measurements for individual crystals or crystals that have been double-dated using apatite fission track and (U-Th)/He.

Acknowledgments
We thank C. Fillon and P. Vermeesch for stimulating discussions and K. Gallagher and C. Mark for constructive reviews. We also thank M. G. Fellin for editorial support. Data used in this study can be obtained from Schwartz et al. (2017). This study was supported by NERC (NE/N015479/1). J. D. was supported by the China Geological Survey (DD20160027) and the Fundamental Research Funds for the Central Universities (292016004).

References

Ault, A. K., & Flowers, R. M. (2012). Is apatite U-Th zonation information necessary for accurate interpretation of apatite (U-Th)/He thermochronometry data? *Geochimica et Cosmochimica Acta*, *79*, 60–78. https://doi.org/10.1016/j.gca.2011.11.037

Ault, A. K., Flowers, R. M., & Bowring, S. A. (2009). Phanerozoic burial and unroofing history of the western Slave craton and Wopmay orogen from apatite (U-Th)/He thermochronometry. *Earth and Planetary Science Letters*, *284*(1–2), 1–11.

Beucher, R., Brown, R. W., Roper, S., Stuart, F., & Persano, C. (2013). Natural age dispersion arising from the analysis of broken crystals: Part II. Practical application to apatite (U–Th)/He thermochronometry. *Geochimica et Cosmochimica Acta*, *120*, 395–416. https://doi.org/10.1016/j.gca.2013.05.042

Brown, R. W., Beucher, R., Roper, S., Persano, C., Stuart, F., & Fitzgerald, P. (2013). Natural age dispersion arising from the analysis of broken crystals. Part I: Theoretical basis and implications for the apatite (U–Th)/He thermochronometer. *Geochimica et Cosmochimica Acta*, *122*, 478–497. https://doi.org/10.1016/j.gca.2013.05.041

Carter, A., & Gallagher, K. (2004). Characterising the significance of provenance on the inference of thermal history models from apatite fission track data—A synthetic data study. In M. Bernet & C. Spiegel (Eds.), *Detrital thermochronology—Provenance analysis, exhumation, and landscape evolution of mountain belts* (Vol. 378, pp. 7–23). Boulder, Colorado: Geological Society of America Special Paper.

Cecil, M. R., Saleeby, Z., Saleeby, J., & Farley, K. A. (2014). Pliocene-Quaternary subsidence and exhumation of the southeastern San Joaquin Basin, California, in response to mantle lithosphere removal. *Geosphere*, *10*(1), 129–147. https://doi.org/10.1130/GES00882.1

Cederbom, C. E., van der Beek, P., Schlunegger, F., Sin- clair, H., & Oncken, O. (2011). Rapid, extensive erosion of the North Alpine foreland basin at 5–4 Ma: Climatic, tectonic and geodynamic forcing on the European Alps. *Basin Research*, *23*(5), 528–550. https://doi.org/10.1111/j.1365-2117.2011.00501.x

Danišík, M., McInnes, B. I., Kirkland, C. L., McDonald, B. J., Evans, N. J., & Becker, T. (2017). Seeing is believing: Visualization of He distribution in zircon and implications for thermal history reconstruction on single crystals. *Science Advances*, *3*(2), e1601121). https://doi.org/10.1126/sciadv.1601121

Djimbi, D. M., Gautheron, C., Roques, J., Tassan-Got, L., Gerin, C., & Simoni, E. (2015). Impact of apatite chemical composition on (U-Th)/He thermochronometry: An atomistic point of view. *Geochimica et Cosmochimica Acta*, *167*, 162–176. https://doi.org/10.1016/j.gca.2015.06.017

Dodson, M. H. (1973). Closure temperature in cooling geochronological and petrological systems. *Contributions to Mineralogy and Petrology*, *40*(3), 259–274. https://doi.org/10.1007/BF00373790

Evans, N. J., McInnes, B. I. A., McDonald, B., Danišík, M., Becker, T., Vermeesch, P., et al. (2015). An in situ technique for (U–Th–Sm)/He and U–Pb double dating. *Journal of Analytical Atomic Spectrometry*, *30*(7), 1636–1645. https://doi.org/10.1039/C5JA00085H

Farley, K. A., Shuster, D. L., & Ketcham, R. A. (2011). U and Th zonation in apatite observed by laser ablation ICPMS, and implications for the (U-Th)/He system. *Geochimica et Cosmochimica Acta*, *75*(16), 4515–4530. https://doi.org/10.1016/j.gca.2011.05.020

Farley, K. A., Wolf, R. A., & Silver, L. T. (1996). The effects of long alpha-stopping distances on (U-Th)/He ages. *Geochimica et Cosmochimica Acta*, *60*(21), 4223–4229. https://doi.org/10.1016/S0016-7037(96)00193-7

Fillon, C., Gautheron, C., & van der Beek, P. (2013). Oligocene-Miocene burial and exhumation of the Southern Pyrenean foreland quantified by low-temperature thermochronology. *Journal of the Geological Society*, *170*(1), 67–77. https://doi.org/10.1144/jgs2012-051

Fitzgerald, P. G., Baldwin, S. L., Webb, L. E., & O'Sullivan, P. B. (2006). Interpretation of (U-Th)/He single grain ages from slowly cooled crustal terranes: A case study from the Transantarctic Mountains of southern Victoria Land. *Chemical Geology*, *225*(1-2), 91–120. https://doi.org/10.1016/j.chemgeo.2005.09.001

Flowers, R. M. (2009). Exploiting radiation damage control on apatite (U-Th)/He dates in cratonic regions. *Earth and Planetary Science Letters*, *277*(1–2), 148–155.

Flowers, R. M., & Kelley, S. A. (2011). Interpreting data dispersion and "inverted" dates in apatite (U-Th)/He and fission-track datasets: An example from the US midcontinent. *Geochimica et Cosmochimica Acta*, *75*(18), 5169–5186. https://doi.org/10.1016/j.gca.2011.06.016

Flowers, R. M., Ketcham, R. A., Shuster, D. L., & Farley, K. A. (2009). Apatite (U-Th)/He thermochronometry using a radiation damage accumulation and annealing model. *Geochimica et Cosmochimica Acta*, *73*(8), 2347–2365. https://doi.org/10.1016/j.gca.2009.01.015

Fox, M., Herman, F., Kissling, E., & Willett, S. D. (2015). Rapid exhumation in the Western Alps driven by slab detachment and glacial erosion. *Geology*, *43*(5), 379–382. https://doi.org/10.1130/G36411.1

Fox, M., McKeon, R. E., & Shuster, D. L. (2014). Incorporating 3-D parent nuclide zonation for apatite 4He/3He thermochronometry: An example from the Appalachian Mountains. *Geochemistry, Geophysics, Geosystems*, *15*, 4217–4229. https://doi.org/10.1002/2014GC005464

Fox, M., & Shuster, D. L. (2014). The influence of burial heating on the (U–Th)/He system in apatite: Grand Canyon case study. *Earth and Planetary Science Letters*, *397*, 174–183. https://doi.org/10.1016/j.epsl.2014.04.041

Fox, M., Tripathy-Lang, A., Shuster, D. L., Winn, C., Karlstrom, K., & Kelly, S. (2017). Westernmost Grand Canyon incision: Testing thermochronometric resolution. *Earth and Planetary Science Letters*, *474*, 248–256. https://doi.org/10.1016/j.epsl.2017.06.049

Gallagher, K. (2012). Transdimensional inverse thermal history modeling for quantitative thermochronology. *Journal of Geophysical Research*, *117*, B02408. https://doi.org/10.1029/2011JB008825

Gastil, R. G., DeLisle, M., & Morgan, J. R. (1967). Some effects of progressive metamor-phism on zircons. *Geological Society of America Bulletin*, *78*(7), 879–906.

Gautheron, C., Barbarand, J., Ketcham, R. A., Tassan-Got, L., van der Beek, P., Pagel, M., et al. (2013). Chemical influence on α-recoil damage annealing in apatite: Implications for (U–Th)/He dating. *Chemical Geology*, *351)*, 257–267.

Gautheron, C., Tassan-Got, L., Barbarand, J., & Pagel, M. (2009). Effect of alpha-damage annealing on apatite (U-Th)/He thermochronology. *Chemical Geology*, *266*(3-4), 157–170. https://doi.org/10.1016/j.chemgeo.2009.06.001

Gautheron, C., Tassan-Got, L., Ketcham, R. A., & Dobson, K. J. (2012). Accounting for long alpha-particle stopping distances in (U-Th-Sm)/He geochronology: 3D modeling of diffusion, zoning, implantation, and abrasion. *Geochimica et Cosmochimica Acta*, *96*, 44–56. https://doi.org/10.1016/j.gca.2012.08.016

Gerin, C., Gautheron, C., Oliviero, E., Bachelet, C., Djimbi, D. M., Seydoux-Guillaume, A. M., et al. (2017). Influence of vacancy damage on He diffusion in apatite, investigated at atomic to mineralogical scales. *Geochimica et Cosmochimica Acta*, *197*, 87–103. https://doi.org/10.1016/j.gca.2016.10.018

Green, P. F., Crowhurst, P. V., Duddy, I. R., Japsen, P., & Holford, S. P. (2006). Conflicting (U–Th)/He and fission track ages in apatite: Enhanced He retention, not anomalous annealing behaviour. *Earth and Planetary Science Letters*, *250*(3-4), 407–427. https://doi.org/10.1016/j.epsl.2006.08.022

Green, P. F., & Duddy, I. R. (2012). Thermal history reconstruction in sedimentary basins using apatite fission-track analysis and related techniques. In B. A. Vining & S. C. Pickering (Eds.), *Petroleum Geology: From Mature Basins to New Frontiers - Proceedings of the 7th Petroleum Conference*, *Geological Society, London* (pp. 633–644). https://doi.org/10.1144/0070633

Green, P. F., & Duddy, I. R. (2018). Apatite (U-Th-Sm)/He thermochronology on the wrong side of the tracks. *Chemical Geology*, *488*, 21–33. https://doi.org/10.1016/j.chemgeo.2018.04.028

Hourigan, J. K., Reiners, P. W., & Brandon, M. T. (2005). U-Th zonation-dependent alpha-ejection in (U-Th)/He chronometry. *Geochimica et Cosmochimica Acta*, *69*(13), 3349–3365.

Ketcham, R. A. (2005). Forward and inverse modeling of low-temperature thermochronometry data. *Reviews in Mineralogy and Geochemistry*, *58*(1), 275–314. https://doi.org/10.2138/rmg.2005.58.11

Ketcham, R. A., Carter, A., Donelick, R. A., Barbarand, J., & Hurford, A. J. (2007). Improved modeling of fission-track annealing in apatite. *American Mineralogist*, *92*(5-6), 799–810. https://doi.org/10.2138/am.2007.2281

McDannell, K. T., Zeitler, P. K., Janes, D. G., Idleman, B. D., & Fayon, A. K. (2018). Screening apatites for (U-Th)/He thermochronometry via continuous ramped heating: He age components and implications for age dispersion. *Geochimica et Cosmochimica Acta*, *223*, 90–106. https://doi.org/10.1016/j.gca.2017.11.031

McKeon, R. E., Zeitler, P. K., Pazzaglia, F. J., Idleman, B. D., & Enkelmann, E. (2014). Decay of an old orogen: Inferences about Appalachian landscape evolution from low-temperature thermochronology. *Bulletin*, *126*(1-2), 31–46.

Murray, K. E., Orme, D. A., & Reiners, P. W. (2014). Effects of U-Th-rich grain boundary phases on apatite helium ages. *Chemical Geology*, *390*, 135–151.

Nielsen, S. B., Clausen, O. R., & McGregor, E. (2017). Basin% Ro: A vitrinite reflectance model derived from basin and laboratory data. *Basin Research*, *29*, 515–536. https://doi.org/10.1111/bre.12160

Powell, J. W., Schneider, D. A., & Issler, D. R. (2018). Application of multi-kinetic apatite fission track and (U-Th)/He thermochronology to source rock thermal history: a case study from the Mackenzie Plain, NWT, Canada. *Basin Research*, *30*, 497–512. https://doi.org/10.1111/bre.12233

Recanati, A., Gautheron, C., Barbarand, J., Missenard, Y., Pinna-Jamme, R., Tassan-Got, L., et al. (2017). Helium trapping in apatite damage: Insights from (U-Th-Sm)/He dating of different granitoid lithologies. *Chemical Geology*, *470*, 116–131. https://doi.org/10.1016/j.chemgeo.2017.09.002

Schwartz, S., Gautheron, C., Audin, L., Dumont, T., Nomade, J., Barbarand, J., et al. (2017). Foreland exhumation controlled by crustal thickening in the Western Alps. *Geology*, *45*(2), 139–142. https://doi.org/10.1130/G38561.1

Shuster, D. L., & Farley, K. A. (2004). $^{4}He/^{3}He$ thermochronometry. *Earth and Planetary Science Letters*, *217*(1-2), 1–17. https://doi.org/10.1016/S0012-821X(03)00595-8

Shuster, D. L., & Farley, K. A. (2009). The influence of artificial radiation damage and thermal annealing on helium diffusion kinetics in apatite. *Geochimica et cosmochimica Acta*, *73*(1), 183–196. https://doi.org/10.1016/j.gca.2008.10.013

Shuster, D. L., Flowers, R. M., & Farley, K. A. (2006). The influence of natural radiation damage on helium diffusion kinetics in apatite. *Earth and Planetary Science Letters*, *249*(3-4), 148–161. https://doi.org/10.1016/j.epsl.2006.07.028

Sinclair, H. D., Coakley, B. J., Allen, P. A., & Watts, A. B. (1991). Simulation of foreland basin stratigraphy using a diffusion model of mountain belt uplift and erosion: an example from the central Alps, Switzerland. *Tectonics*, *10*(3), 599–620. https://doi.org/10.1029/90TC02507

Spiegel, C., Kohn, B., Belton, D., Berner, Z., & Gleadow, A. (2009). Apatite (U-Th-Sm)/He thermochronology of rapidly cooled samples: The effect of He implantation. *Earth and Planetary Science Letters*, *285*(1-2), 105–114. https://doi.org/10.1016/j.epsl.2009.05.045

Thomson, S. N., Reiners, P. W., Hemming, S. R., & Gehrels, G. E. (2013). The contribution of glacial erosion to shaping the hidden landscape of East Antarctica. *Nature Geoscience*, *6*(3), 203–207. https://doi.org/10.1038/ngeo1722

Tian, Y., Vermeesch, P., Danišík, M., Condon, D. J., Chen, W., Kohn, B., & Rittner, M. (2017). LGC-1: A zircon reference material for in-situ (U-Th)/He dating. *Chemical Geology*, *454*, 80–92. https://doi.org/10.1016/j.chemgeo.2017.02.026

Tripathy-Lang, A., Hodges, K. V., Monteleone, B. D., & Soest, M. C. (2013). Laser (U-Th)/He thermochronology of detrital zircons as a tool for studying surface processes in modern catchments. *Journal of Geophysical Research: Earth Surface*, *118*, 1333–1341. https://doi.org/10.1002/jgrf.20091

Vermeesch, P., Seward, D., Latkoczy, C., Wipf, M., Günther, D., & Baur, H.m. (2007). α-Emitting mineral inclusions in apatite, their effect on (U-Th)/He ages, and how to reduce it. *Geochimica et Cosmochimica Acta*, *71*(7), 1737–1746. https://doi.org/10.1016/j.gca.2006.09.020

Vermeesch, P., Sherlock, S. C., Roberts, N. M., & Carter, A. (2012). A simple method for in-situ U-Th-He dating. *Geochimica et Cosmochimica Acta*, *79*, 140–147. https://doi.org/10.1016/j.gca.2011.11.042

Vermeesch, P., & Tian, Y. (2014). Thermal history modelling: HeFTy vs. QTQt. *Earth-Science Reviews*, *139*, 279–290. https://doi.org/10.1016/j.earscirev.2014.09.010

Willett, C. D., Fox, M., & Shuster, D. L. (2017). Helium-based model for the effects of radiation damage annealing on helium diffusion kinetics in apatite. *Earth and Planetary Science Letters*, *477*, 195–204. https://doi.org/10.1016/j.epsl.2017.07.047

Winn, C., Karlstrom, K. E., Shuster, D. L., Kelley, S., & Fox, M. (2017). 6 Ma age of carving Westernmost Grand Canyon: Reconciling geologic data with combined AFT,(U–Th)/He, and 4He/3He thermochronologic data. *Earth and Planetary Science Letters*, *474*, 257–271. https://doi.org/10.1016/j.epsl.2017.06.051

Wolf, R. A., Farley, K. A., & Kass, D. M. (1998). Modeling of the temperature sensitivity of the apatite (U-Th)/He thermochronometer. *Chemical Geology*, *148*(1-2), 105–114. https://doi.org/10.1016/S0009-2541(98)00024-2

Wolf, R. A., Farley, K. A., & Silver, L. T. (1996). Helium diffusion and low-temperature thermochronometry of apatite. *Geochimica et Cosmochimica Acta*, *60*(21), 4231–4240. https://doi.org/10.1016/S0016-7037(96)00192-5

Zeitler, P. K., Enkelmann, E., Thomas, J. B., Watson, E. B., Ancuta, L. D., & Idleman, B. D. (2017). Solubility and trapping of helium in apatite. *Geochimica et Cosmochimica Acta*, *209*, 1–8. https://doi.org/10.1016/j.gca.2017.03.041

Zeitler, P. K., Herczeg, A. L., McDougall, I., & Honda, M. (1987). U-Th-He dating of apatite: A potential thermochronometer. *Geochimica et Cosmochimica Acta*, *51*(10), 2865–2868. https://doi.org/10.1016/0016-7037(87)90164-5